



The quasicrystalline phase formation in Al–Cu–Cr alloys produced by mechanical alloying

T.A. Sviridova^{a,*}, A.P. Shevchukov^a, E.V. Shelekhov^a, D.L. Diakonov^b, V.V. Tcherdyntsev^a, S.D. Kaloshkin^a

^a National University of Science and Technology "MISIS", Moscow 119049, Russia

^b Bardin Central Research Institute for the Iron and Steel Industry, Moscow 105005, Russia

ARTICLE INFO

Article history:

Received 4 July 2010

Received in revised form

26 November 2010

Accepted 13 December 2010

Available online 21 December 2010

Keywords:

Quasicrystals

Mechanical alloying

Intermetallics

X-ray diffraction

Scanning electron microscopy

Transmission electron microscopy

ABSTRACT

Almost single-phase decagonal quasicrystal with periodicity of 1.26 nm along 10-fold axis was produced in Al₆₉Cu₂₁Cr₁₀ and Al_{72.5}Cu_{16.5}Cr₁₁ alloys using combination of mechanical alloying (MA) and subsequent annealing. Phase transformations of as-milled powders depending on annealing temperature in the range of 200–800 °C are examined. Since the transformations can be explained based on kinetic and thermodynamic reasons it seems that applied technique (short preliminary MA followed by the annealing) permits to produce the equilibrium phases rather than metastable ones.

© 2010 Elsevier B.V. All rights reserved.

1. Introduction

The quasicrystals (QC) have very specific and perspective properties and can be used by itself and as a filler of various composite materials. But the most known and widely applied stable Al–Cu–Fe quasicrystal has a poor corrosion resistance [1] that may be improved by substituting chromium for iron similarly to stainless steels. The MA combined with the annealing proved to be quite successful way to produce quasicrystalline phases [2–4] though narrow homogeneity regions of QCs provide certain difficulties caused by an unpredictable change of chemical composition during MA.

At the beginning of this work there were no reliable data about Al–Cu–Cr phase diagram (they were out of date and contradictory) but in the last few years the systematic investigations of the phase diagram were carried out [5,6] in which the compositions of several compounds were determined (Fig. 1), among them cubic Ψ -Al₆₅Cu₂₅Cr₁₀, φ -Al_{70.5}Cu₁₈Cr_{11.5} with unidentified structure, and stable up to 638 °C fcc λ -Al₆₁Cu_{35.5}Cr_{3.5} [5]. It should be noted that the up-to-date version of the Al–Cu–Cr phase diagram below 700 °C has not been reported yet.

There are several works where different QCs in Al–Cu–Cr system were produced by various ways. The icosahedral quasicrystal (IQC) Al₆₅Cu₂₀Cr₁₅ obtained by rapid solidification [7–9] was found to be a metastable phase [10] and can coexist with various compounds [11]. The IQC of the same composition was prepared by prolonged MA with a subsequent short-term annealing [12]. Almost single-phase IQCs were obtained at several compositions by splat [10,13,14] or rapid quenching [15–17]. In [18] two (primitive and face-centered) IQCs and decagonal quasicrystal (DQC), all at various compositions, were observed by transmission electron microscopy in separate selected areas of a multiphase composite. DQCs with two different periodicities of 1.24 nm and 3.78 nm were found in [19,20].

The main purpose of this work was to select mixtures allowing to produce Al–Cu–Cr quasicrystalline phase by MA so we have tested most of reported compositions. While comparing the vast phase analysis data we shall try to reveal some features of intermetallics formation during annealing of as-milled blends. The phase transformations proceeded in each alloy under study will discuss in more detail somewhere else.

2. Materials and methods

The mixtures of elemental powders Al (purity 98.0%, powder size ~250 μ m), Cu (99.5%, ~30–50 μ m) and Cr (98.5%, ~30–50 μ m) were mechanically alloyed in Ar atmosphere using the AGO-2M ball mill at rotational frequency 620 rpm

* Corresponding author at: National University of Science and Technology "MISIS", Center of composites materials, Leninsky pr., 4, 119049, Moscow, Russian Federation, Russia. Tel.: +74959550163; fax: +74956384595.

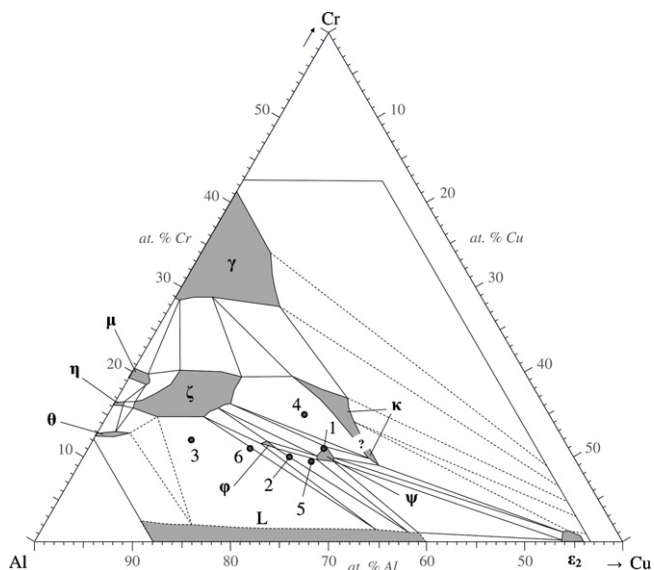


Fig. 1. Isothermal cross-section of Al–Cu–Cr phase diagram at 700 °C [5] and nominal alloys compositions: (1) $\text{Al}_{65}\text{Cu}_{24}\text{Cr}_{11}$, (2) $\text{Al}_{69}\text{Cu}_{21}\text{Cr}_{10}$, (3) $\text{Al}_{78}\text{Cu}_{10}\text{Cr}_{12}$, (4) $\text{Al}_{65}\text{Cu}_{20}\text{Cr}_{15}$, (5) $\text{Al}_{67}\text{Cu}_{23.5}\text{Cr}_{9.5}$, and (6) $\text{Al}_{72.5}\text{Cu}_{16.5}\text{Cr}_{11}$.

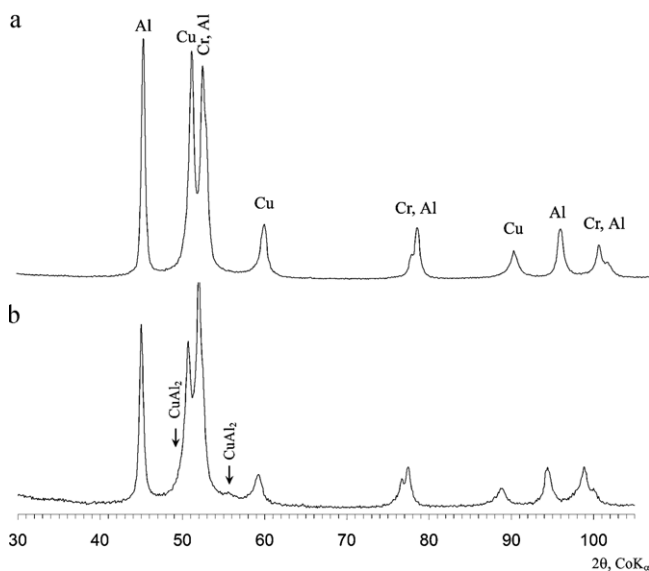


Fig. 2. XRD patterns and phase composition of as-milled: (a) (2) and (b) (5) mixtures subjected to 1 and 2 h of MA respectively.

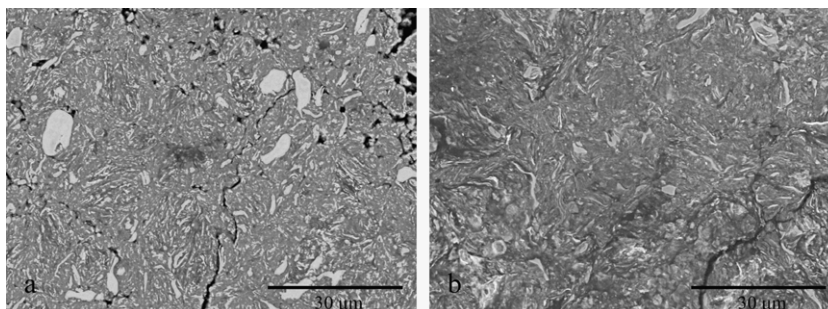


Fig. 3. SEM images of (a) (2) and (b) (6) mixtures for 1 and 2 h of MA respectively.

and centrifugal acceleration 210 m/s². Three alloy compositions (1) $\text{Al}_{65}\text{Cu}_{24}\text{Cr}_{11}$, (2) $\text{Al}_{69}\text{Cu}_{21}\text{Cr}_{10}$, (3) $\text{Al}_{78}\text{Cu}_{10}\text{Cr}_{12}$ were chosen following [18] and correspond to two IQCs and DQC. Proportions of the alloy (4) $\text{Al}_{65}\text{Cu}_{20}\text{Cr}_{15}$ coincide with IQC in [7–11,12] and the last two alloys (5) $\text{Al}_{67}\text{Cu}_{23.5}\text{Cr}_{9.5}$ and (6) $\text{Al}_{72.5}\text{Cu}_{16.5}\text{Cr}_{11}$ have the composition of Ψ - and φ -phases [5] corrected for possible sticking effect of Al and contamination by Fe due to wear of balls and vial walls. The nominal compositions of alloys under study are shown in Fig. 1. The real compositions were measured by X-ray microprobe analysis (scanned area was 1.5 mm²) using SMA-Quanta 3D FEG microscope and did not move aside considerably: Al content was less than nominal one by 1–2 at.%, Cr and Cu deviations were 0.5–1 at.% and about 0.5 at.% Fe was detected.

The duration of MA was 1 h for the first three alloys and 2 h for the last three ones. The powder to ball ratio was 1:10, 200 g of balls (ball bearing steel) were charged in each vial (hardened steel) with filling ratio 35–40%. The 0.2 ml of ethyl alcohol served as a process control agent preventing adhesion of mixtures on work surfaces.

The thermal analysis was done using the microcalorimeter Setaram DSC-111 (mixtures 1–3) and DTA-7 HT thermal analyser (mixtures 4–6) at heating rates of 20 K/min and 100 K/min respectively. As-milled powders were annealed for 1 h at the fixed temperatures in the range of 200–800 °C (with accuracy 5 °C) in a pipe furnace under Ar atmosphere and then air-cooled.

X-ray diffraction (XRD) data were collected with Co K α radiation and treated by some kind of Rietveld algorithm [21]. The QC volume fraction was evaluated by measuring the absolute intensity of almost single-phase quasicrystal with respect to the corundum reference.

Hitachi TM-1000 and JSM-6480LV scanning electron microscopes (SEM) were used to study powder microstructure and elements distribution. The quasicrystalline phase was examined by transmission electron microscope JEM-200CX.

3. Results

3.1. Mechanical alloying

The preliminary MA permits to intermix the components uniformly, increase interphase surfaces and reduce diffusion paths, i.e. facilitate intermetallics formation on a subsequent annealing.

The phase composition of all as-milled blends is quite similar to that in initial state and only slightly depends on milling time. Fig. 2 shows typical XRD patterns after 1 and 2 h of MA. The only visible change in phase composition registered after 2 h was the appearance of a trace amount of CuAl_2 phase. Lattice parameters of initial elements remained constant within a statistical error, showing lack of mutual solubility. The microstrains evaluated from X-ray peaks broadening appeared to be higher (0.3–0.4%) in plastic and easily deformed Al and Cu whereas in harder Cr they scarcely attained to 0.1%.

The powder size of all mechanically alloyed mixtures was several tens of micrometers. Fig. 3 shows microstructures of the mixtures (2) and (6) subjected to 1 and 2 h of MA respectively. In the both pictures there are clearly visible hard Cr-particles inside closely intermixed Al and Cu components. In the course of MA Cr-particles are comminuted, flattened and as a result elongated. After 2 h the Cr-layers reduce to about 1 μm in thickness though some Cr-particles remain equiaxed and about several microns in size. The Cu and Al layers are unresolved in element distribution map so they are less than 1 μm thick. The similar fine structure with submicron-sized layers was clearly resolved by Z-contrast in binary Al–Cu mechanically alloyed mixtures [22].

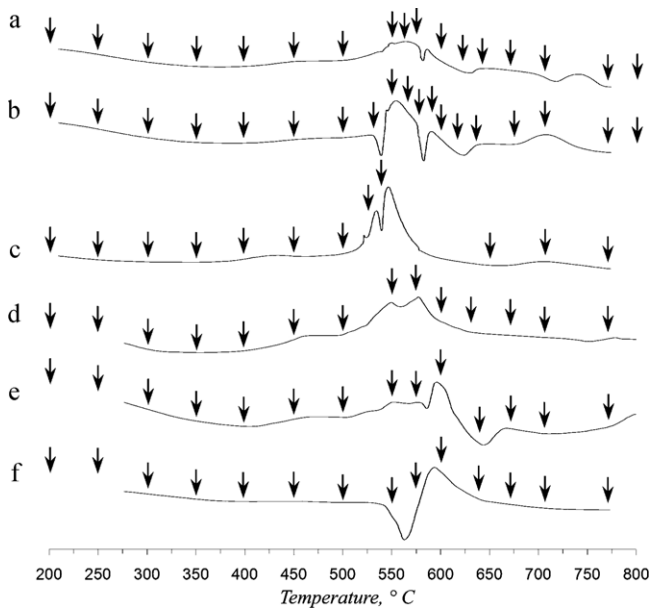


Fig. 4. DSC (a–c) and DTA (d–f) curves and marked by arrows annealing temperatures of (a) (1), (b) (2), (c) (3), (d) (4), (e) (5) and (f) (6) mixtures subjected to MA.

3.2. Annealing

The heating of as-milled powders causes diffusion interaction of components that results in phase transformations controlled by both thermodynamic and kinetic factors. It was preliminarily

checked that the phase composition on annealing at 570 °C reaches a stationary state for 15 min so we believe that 1 h is sufficient to achieve the steady state above 500 °C.

The thermal analysis of the powders reveals besides several exothermic effects related to intermediate phases formation irreversible endothermic transformations (Fig. 4) that practically coincide with binary Cu–Al eutectic and CuAl_2 peritectic decomposition. So they are most probably induced by partial melting that can accelerate components diffusivities.

To reveal the character of components interaction the phase composition depending on annealing temperature is examined and schematically shown in Fig. 5. Annealing temperatures are pointed out by arrows in Fig. 4. Some of respective XRD patterns are presented in Fig. 6. The descent of thermal curves at 200–250 °C corresponds to the “tail” of exothermic peak related to the CuAl_2 phase formation accompanied by almost complete Cu depletion but the content of CuAl_2 phase surprisingly grows up to 400–450 °C. The CuAl_2 phase is stable up to 600 °C and vanishes above this temperature in all alloys except (3) where it remains in compliance with the phase diagram.

The chromium gradually dissolves with the elevation of annealing temperature. At 200 °C it contributes to the formation of cubic $\lambda\text{-Al}_{61}\text{Cu}_{35}\text{Cr}_4$ phase [5] that at 350–400 °C is partly or completely replaced by $\varphi\text{-Al}_{71}\text{Cu}_{18}\text{Cr}_{12}$ phase [5]. Above 500 °C the λ -phase content begins to grow up whereas at 600–640 °C the λ -phase decomposes in all alloys except (6).

The ternary φ -phase arises in all alloys giving slight exothermic peak at 350–450 °C and at the 550 °C its content becomes significant. The maximum amount of the phase (~90–95 vol.%) is achieved in (2) and (6) alloys annealed at 635 °C and with the growth of annealing temperature its content either remains the

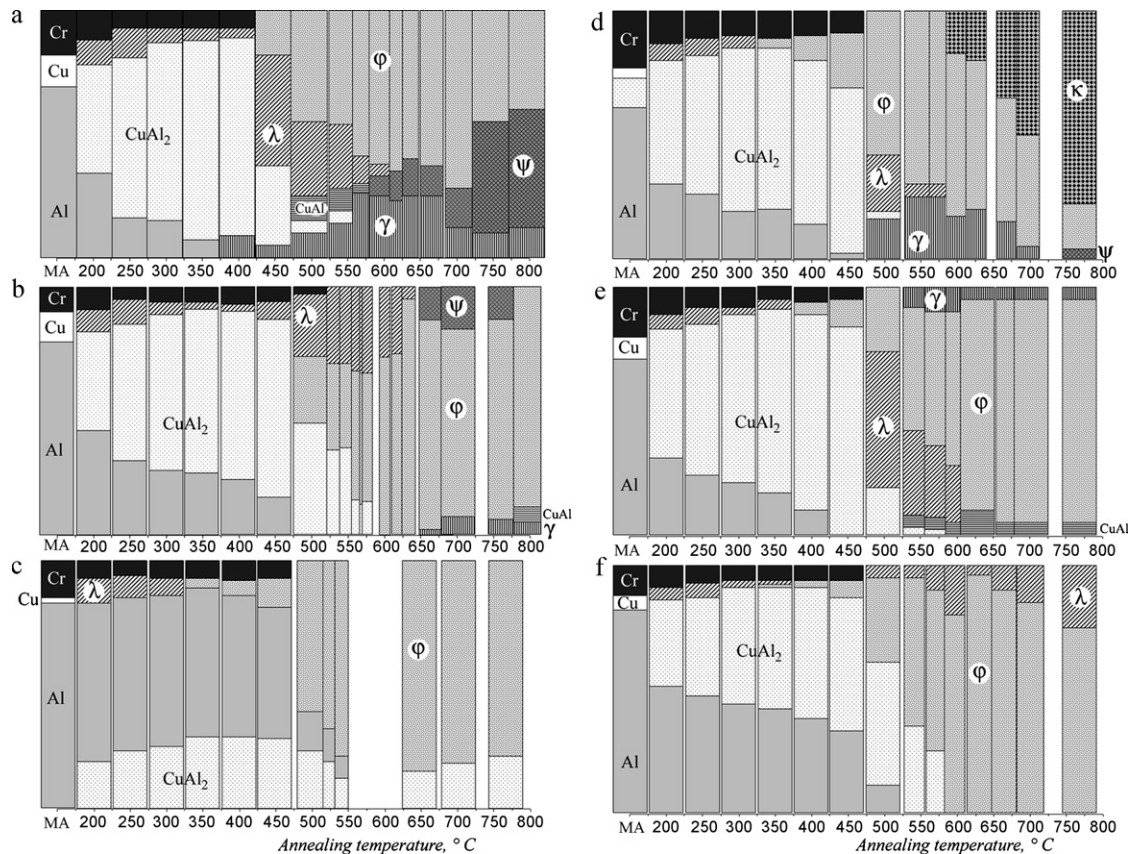


Fig. 5. Schematic phase composition of mechanically alloyed and annealed mixtures: (1) a, (2) b, (3) c, (4) d, (5) e and (6) f. The following phases notations are used: $\lambda\text{-Al}_{61}\text{Cu}_{35}\text{Cr}_4$; $\Psi\text{-Al}_{65}\text{Cu}_{25}\text{Cr}_{10}$; $\varphi\text{-Al}_{71}\text{Cu}_{18}\text{Cr}_{12}$; γ —practically binary Al–Cu phase with a structure closely related to γ -brass; $\eta_2\text{-CuAl}$ —low-temperature monoclinic CuAl; κ —phase near the composition of $\text{Al}_{62}\text{Cu}_{23}\text{Cr}_{15}$ (see Fig. 1).

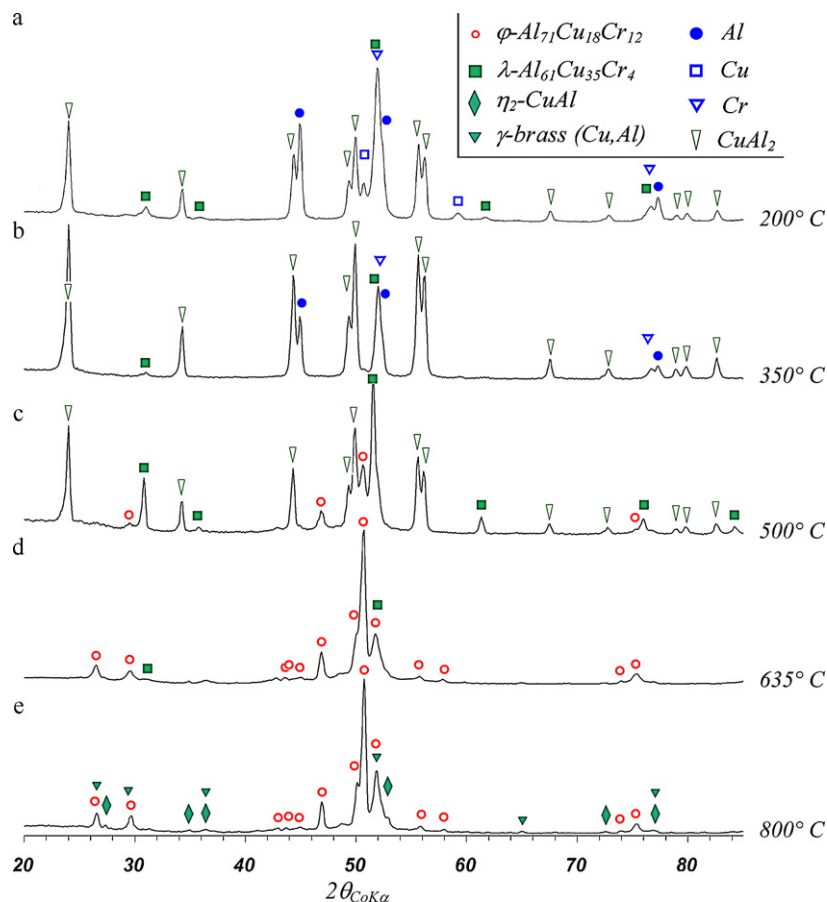


Fig. 6. XRD pattern of alloy (2) annealed at (a) 200 °C, (b) 350 °C, (c) 500 °C, (d) 635 °C and (e) 800 °C.

same or slightly falls with the exception of mixture (4) where the φ -phase almost entirely transforms into equilibrium κ -phase [5]. The XRD pattern of the annealed at 635 °C alloy (2) (*sample (2)-635*) is practically the same with that of the φ -phase in [5] (Fig. 6d). The structure of this phase is hitherto not determined though its XRD pattern has distinct features of decagonal quasicrystals in the similar systems. In addition, the same phase was formed in [12] after short-term annealing of $\text{Al}_{65}\text{Cu}_{20}\text{Cr}_{15}$ mixture subjected to long-term MA.

The Patterson function of DQC and its Fourier transform have two non-equivalent types of 2-fold axes (2P and 2D), which alternate every 18° by rotation about the 10-fold axis, and many pseudo 2-, 3- and 5-fold axes inherited from IQC [23,24]. The electron diffraction patterns (EDPs) of the *sample (2)-635* (Fig. 7a and b) are

typical for 2P and 2D axes and were taken by rotation through 18° about 10-fold axis denoted as 10 in Fig. 7a and b. We failed to obtain the EDP with 10-fold symmetry but succeeded in measuring the angles between 2P and pseudo 5- (Fig. 7c) and 3-fold axes, which proved to be 28° and 10.5° respectively. These angles are very close to that of DQC in Al–Fe and Al–Cr systems [24,25]. The translation along 10-fold axis is about 1.26 nm so the φ -phase belongs to D_3 family of DQCs [26].

The SEM analysis confirms almost single-phase state of the *sample (2)-635*. The φ -phase composition measured in several points by microprobe analysis appeared to be $\text{Al}_{71.4}\text{Cu}_{19.2}\text{Cr}_{9.4}$ that slightly differs from Ref. [5]. The minor phase has the $\text{Al}_{76.1}\text{Cu}_{9.0}\text{Cr}_{14.9}$ composition that corresponds to DQC in [18]. It should be noted that certain of the XRD patterns have some weak unidentified reflec-

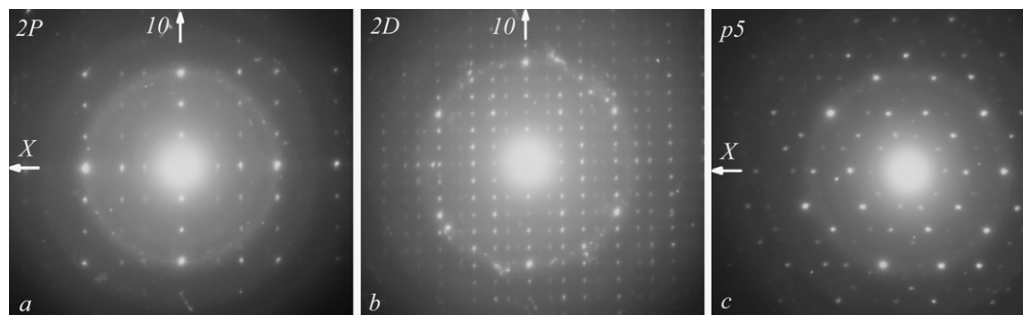


Fig. 7. EDPs of the φ -phase taken along (a) 2P, (b) 2D and (c) pseudo 5-fold axes (p5). Sample rotations needed to transfer from a to: b—18° around axis 10; c—28° around X direction.

tions. Their analysis shows that there are at least two unknown phases near the composition region under study. Maximum content of the one of them is detected on annealing at 705 °C in alloys (1) and (2).

4. Discussion

During MA the elemental blends form inhomogeneous but closely intermixed structure, which is characterized by alternating Cu and Al layers about 1 μm thick with embedded coarse (1–10 μm) Cr-particles. The large random scatter in composition between particles enhances the number of phases forming on annealing since the diffusion interaction between separated particles is severely retarded. The durable MA levels off sporadic deviations of chemical composition of individual particles from average one, i.e. leads to more homogeneous powder state. In our case the 2 h of MA are obviously insufficient for close intermixing of Cr with Cu–Al matrix and so there is no visible influence of milling time on subsequent phase transformations.

The heating of these blends at temperatures below 400–450 °C stimulates the formation of CuAl₂ and almost binary λ-Al₆₁Cu₃₅Cr₄ phases. There are some reasons for these phases to appear. The Al/Cu and Al/Cr enthalpies of mixing are negative unlike the Cu/Cr one (it can be deduced from diagrams appearance), i.e. Cu and Cr have no thermodynamic impulse to react. There is no full set of data on components diffusivities but according to [27,28] it can be inferred that the diffusion coefficient of Cu in Al is appreciably greater than that of Al in Cu and the diffusivity of Cu in Al notably surpasses that of Cr in Al. So the interdiffusion is controlled by diffusivity of transition metals and Cu is the most mobile species. The low hardnesses and high plasticities of Al and Cu facilitate their mutual mechanical and then diffusion intermixing owing to expansion of interphase surface and reduction of diffusion paths. Thus both thermodynamic and kinetic factors make more preferable interaction between Al and Cu.

It seems that at 200–250 °C very thin Cu-layers (5–10 nm) persist and gradually dissolve in surrounding Al but the change in ultrafine phase content is undetectable by XRD. It is likely as well that primarily formed CuAl₂ streaks are also superdispersed and exist in latent state as regards XRD. As the recrystallization of CuAl₂-phase proceeds its apparent volume fraction increases and approaches the true one.

At low temperatures, when Cr-diffusivity is weak, the λ-phase with low Cr-content can form on the boundaries of Cr-particles. At elevated temperatures the formation of enriched by Cr φ-phase occurs and the content of λ-phase decreases. And, as phase diagram prescribes, at higher temperatures λ-phase appears again. The high concentration of grain boundaries at MA provides easy paths for low-temperature diffusion [22] and can promote Cr-dissolution. Above 600 °C the diffusion mobility of Cr is enough to achieve the homogeneity within powder particle and the number of observable phases is reduced.

It should be emphasized that Cr-dissolution is of crucial importance in establishment of phase equilibrium. The temperature growth gives rise to formation of the phases with gradually increasing Cr content: CuAl₂ is replaced by λ-Al₆₁Cu₃₅Cr₄, then by φ-Al₇₁Cu₁₈Cr₁₂ and at last, for Cr-rich alloy by κ-phase with 16–20 at.% of Cr. Presumably, the appearance of decagonal φ-phase in such a wide composition and temperature range contrary to phase diagram is due to survival of residual fine Cr particles unresolved by XRD. Other likely reasons for the discrepancy with phase

diagram are relatively slow air-cooling from annealing temperature and possible stability of φ-phase down to room temperature.

5. Conclusion

The combination of mechanical alloying and subsequent annealing was used to produce the almost single-phase decagonal quasicrystal in Al–Cu–Cr system. All six compositions under study when being annealed contain different amount of φ-phase (decagonal quasicrystal) and its maximum content (~90–95 vol.%) was achieved in (2) Al₆₉Cu₂₁Cr₁₀ and (6) Al_{72.5}Cu_{16.5}Cr₁₁ alloys after annealing at 635 °C during 1 h. The composition of φ-phase was determined as Al_{71.4}Cu_{19.2}Cr_{9.4} that slightly deviates from [5].

Some features of phase transformations caused by annealing of as-milled blends are considered. It is shown that most of them can be explained based on kinetic and/or thermodynamic reasons and the phase diagram can help to understand the phase evolution. We assume that the short preliminary mechanical alloying with the subsequent annealing permits to produce the equilibrium phases rather than metastable ones.

Acknowledgements

This work was supported by Federal Target Program “Scientific and Scientific-Pedagogical Personnel of Innovative Russia” (State contract P450) and Programme of Creation and Development of the National University of Science and Technology “MISIS”

References

- [1] A. Rüdiger, U. Köster, Mater. Sci. Eng. A 294–296 (2000) 890.
- [2] A.I. Salimon, A.M. Korsunsky, E.V. Shelekhov, T.A. Sviridova, Mater. Sci. Forum 321–324 (2000) 676.
- [3] X. Yong, I.T. Chang, I.P. Jones, J. Alloys Compd. 387 (2005) 128.
- [4] A.I. Salimon, A.M. Korsunsky, S.D. Kaloshkin, V.V. Tcherdyntsev, E.V. Shelekhov, T.A. Sviridova, Mater. Sci. Forum 360–362 (2001) 137–142.
- [5] B. Grushko, B. Przepiórzyński, D. Pavlyuchkov, S. Mi, E. Kowalska-Strzemiłk, M. Surowiec, J. Alloys Compd. 442 (2007) 114.
- [6] B. Grushko, E. Kowalska-Strzemiłk, B. Przepiórzyński, M. Surowiec, J. Alloys Compd. 417 (2006) 121.
- [7] A.-P. Tsai, A. Inoue, T. Masumoto, J. Mater. Sci. Lett. 7 (1988) 322.
- [8] S. Ebalard, F. Spaepen, J. Mater. Res. 5 (1990) 62.
- [9] S. Banerjee, R. Goswami, K. Chattopadhyay, A.K. Raychaudhuri, Phys. Rev. B 52 (1995) 3220.
- [10] H. Selke, P.L. Ryder, Mater. Sci. Eng. A 134 (1991) 917.
- [11] V. Khare, N.P. Lalla, R.S. Tiwari, O.N. Srivastava, J. Mater. Res. 10 (1995) 1905.
- [12] J. Eckert, L. Schultz, K. Urban, Acta Metall. Mater. 39 (1991) 1497–1506.
- [13] P.L. Ryder, H. Selke, J. Non-Cryst. Solids 153–154 (1993) 630.
- [14] H. Selke, P.L. Ryder, Mater. Sci. Eng. A 165 (1993) 81.
- [15] R. Popescu, A. Jianu, M. Mănciu, R. Nicula, R. Manaila, J. Alloys Compd. 221 (1995) 240.
- [16] U. Ponkrat, R. Nicula, A. Jianu, E. Burkel, J. Phys.: Condens. Matter 13 (2001) 549.
- [17] V. Khare, R.S. Tiwari, O.N. Srivastava, Cryst. Res. Technol. 32 (1997) 545.
- [18] Y.H. Qi, Z.P. Zhang, Z.K. Hei, C. Dong, J. Alloys Compounds 285 (1999) 221.
- [19] T. Okabe, J.-I. Furihata, K. Morishita, H. Fujimori, Philos. Magn. Lett. 66 (1992) 259.
- [20] J.S. Wu, X.L. Ma, K.H. Kuo, Philos. Magn. Lett. 73 (1996) 163.
- [21] E.V. Shelekhov, T.A. Sviridova, Met. Sci. Heat Treat. 42 (2000) 309.
- [22] T.A. Sviridova, E.V. Shelekhov, A.P. Shevchukov, P.A. Borisova, The Physics of Metals and Metallography, in press.
- [23] H. Zhang, D.H. Wang, K.H. Kuo, J. Mater. Sci. 24 (1989) 2981.
- [24] K.K. Fung, C.Y. Yang, Y.Q. Zhou, J.G. Zhao, W.S. Zhan, B.G. Shen, Phys. Rev. Lett. 56 (1986) 2060.
- [25] K.Y. Wen, Y.L. Chen, K.H. Kuo, Metall. Trans. A 23 (1992) 2437.
- [26] B. Grushko, T. Velikanova, Comput. Coupling Phase Diagrams Thermochem. 31 (2007) 217.
- [27] C.I. Smithells, Metals Reference Book, Metallurgy, Moscow. Publ., 1980 (in Russian).
- [28] <http://dssp.karelia.ru/~sv/T.p.m.ved/files/Material/Unit%202/2.1.2.htm>.